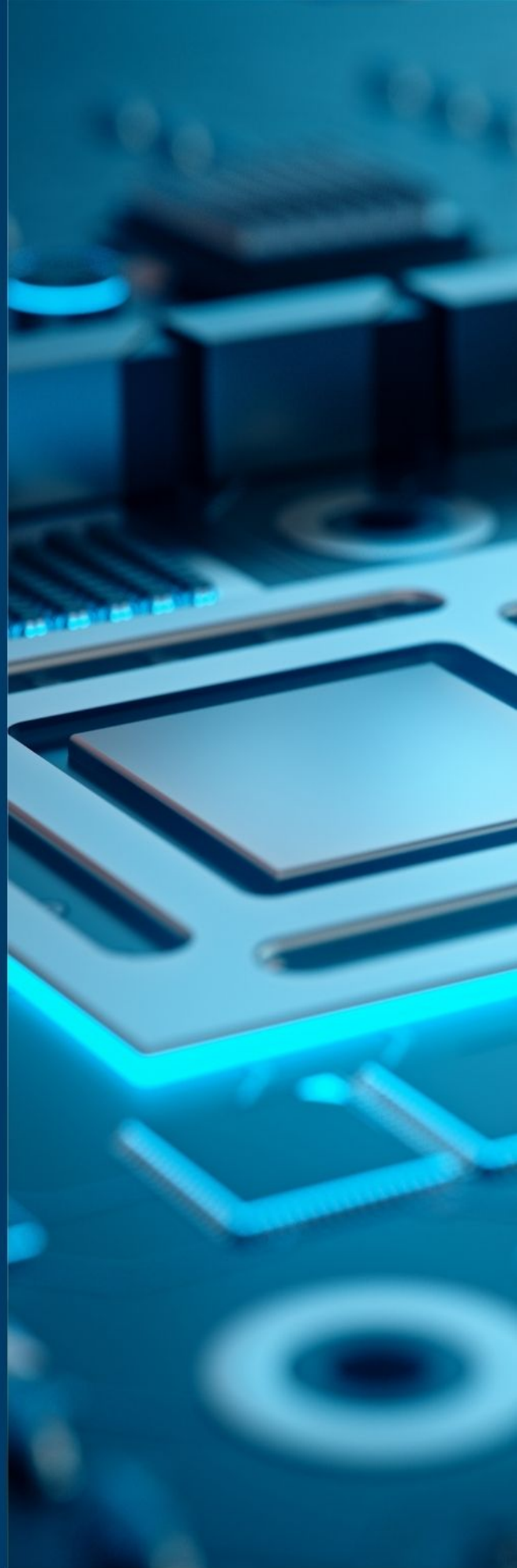# *IET Power Electronics*

Special issue Call for Papers

Be Seen. Be Cited. Submit your work to a new IET special issue

Connect with researchers and experts in your field and share knowledge.

Be part of the latest research trends, faster.

Read more

IET The Institution of Engineering and Technology

Experimental realisation of an AC-link shunt-series power flow controller

Manuel Barragán-Villarejo[1] ✉, José M. Maza-Ortega[1], Fernando Mancilla-David[2], Francisco de Paula García-López[1]

[1]Department of Electrical Engineering, Universidad de Sevilla, Avda. De los Descubrimientos s/n, Sevilla 41092, Spain
[2]Department of Electrical Engineering, University of Colorado Denver, Denver, CO 80217, USA
✉ E-mail: manuelbarragan@us.es

Abstract: Power electronic-based interties in the distribution system are considered an important element for the integration of distributed energy resources. They can provide a series of network services such as active and reactive power control, voltage regulation and harmonic and imbalance compensation that facilitate the integration of these new resources. Despite dc links are usually proposed for this purpose, it is also possible to interconnect radial distribution feeders by means of ac links with direct ac/ac power conversion. This study presents the experimental validation of a current control loop based on feedback linearisation for an ac-link shunt-series power flow controller based on a vector switching matrix converter. The experimental results demonstrate the effectiveness of the proposed control in both steady-state and transient conditions.

1 Introduction

Power electronic devices have become the key to efficiently integrate distributed energy resources (DERs) such as photovoltaic power plants, electric vehicles or energy storage systems [1]. Particularly, the use of flexible links or interties in distribution networks to interconnect adjacent radial feeders, commonly referred to as distribution flexible ac transmission systems (D-FACTS) [2], have demonstrated their potential to maximise the integration of DERs and the efficiency of the distribution network [3]. Among other functionalities, these allow controlling the active and reactive power flows between the interconnected feeders [4], voltage control at the point of common coupling (PCC) [5], active filter functionalities [6] and imbalance compensation in the distribution network.

The most common topologies for this type of interconnections are those based on back-to-back voltage source converters using a dc link. However, some alternative topologies based on direct ac links, e.g. those using a vector switching converter (VeSC) as the constituent power electronic building block, are also of interest owing to their simplicity, the absence of large dc capacitors and lower power rating of the power electronic devices [7]. Among them, the ac-link shunt-series power flow controller (ac-link ShSPFC), presented in [8] and shown on the circuit schematic at the top of Fig. 1, has proven to be the best performing arrangement in terms of increased DERs penetration and reduction of power losses in distribution networks [9]. Several publications have addressed control strategies for VeSC-based D-FACTS. In [10], a modified particle swarm optimisation algorithm is used to obtain the optimal control parameters of an ac-link ShSPFC. Although a fast dynamic response is obtained with a simple control strategy, the active and reactive power flows have a high coupling degree. In [8], two control strategies for independent control of active and reactive power flows between two interconnected buses through an ac-link ShSPFC are presented: classical PI controller and feedback linearisation. Both control strategies are based on the nonlinear averaged model in the *dq* coordinates. However, there are important differences between them that lead to a better performance of the feedback linearisation strategy over the classical PI controller, which are analysed below.

The first strategy decouples and linearises the *dq* model around an operating point. For this, two new duty ratios called d_P and d_Q are defined from the original ones: $[d_1, d_2, d_3]$. These new duty

ratios are strongly related to the power flows managed by the ac-link ShSPFC. In [8], it is shown that d_P mainly affects the active power flow while d_Q affects the reactive power flow in networks with a high X/R ratio. From this relationship, the *dq* model can be linearised, obtaining two single-input single-output (SISO) systems: one for active power (d_P) and the other one for reactive power (d_Q). In this way, a classic proportional–integral (PI) controller can be applied to each SISO system allowing to control the active and reactive power flows managed by the ac-link ShSPFC.

The second control strategy, namely feedback linearisation, is based on controlling the power flows through the VeSC currents formulated in the *dq* axis, i_s^d and i_s^q. For this purpose, an algebraic transformation is proposed in the *dq* domain using two auxiliary variables $[u^d, u^q]$ that allow us to obtain two SISO systems fully decoupled for currents $[i_s^d, i_s^q]$. Thus, a PI controller can be applied to each system and the gains are computed to obtain a first-order response for the closed-loop control system [11]. In order to eliminate the coupling of the currents in the *dq* model, the cancellation of cross-coupling terms is added to the control strategy. Moreover, the injected series voltages by the ac-link ShSPFC are also added to the controller as a feedforward signal to improve its dynamic response. Note that this controller is independent of the X/R ratio because it is designed considering only the ac-link ShSPFC model and controlling the PCC active and reactive power. Based on this discussion, the feedback linearisation strategy is considered to be superior, and is selected for experimental validation. The inner current control loops of this strategy are depicted on the block diagram at the bottom of Fig. 1.

In spite of [8] has defined and simulated this control algorithm, it lacks the corresponding experimental validation required to fully assess its benefits and also limitations related to an actual implementation. Therefore, the main objective of this paper is to experimentally validate the current control strategy based on the feedback linearisation strategy, which has not been previously addressed in the specialised literature. A former study has evaluated the closed-loop operation of an ac-link ShSPFC but supplying a passive load and acting a dynamic voltage restorer [12]. To the best of our knowledge, this paper reports the first experimental validation of the closed-loop operation of an ac-link ShSPFC interconnecting two power systems. Note that the current
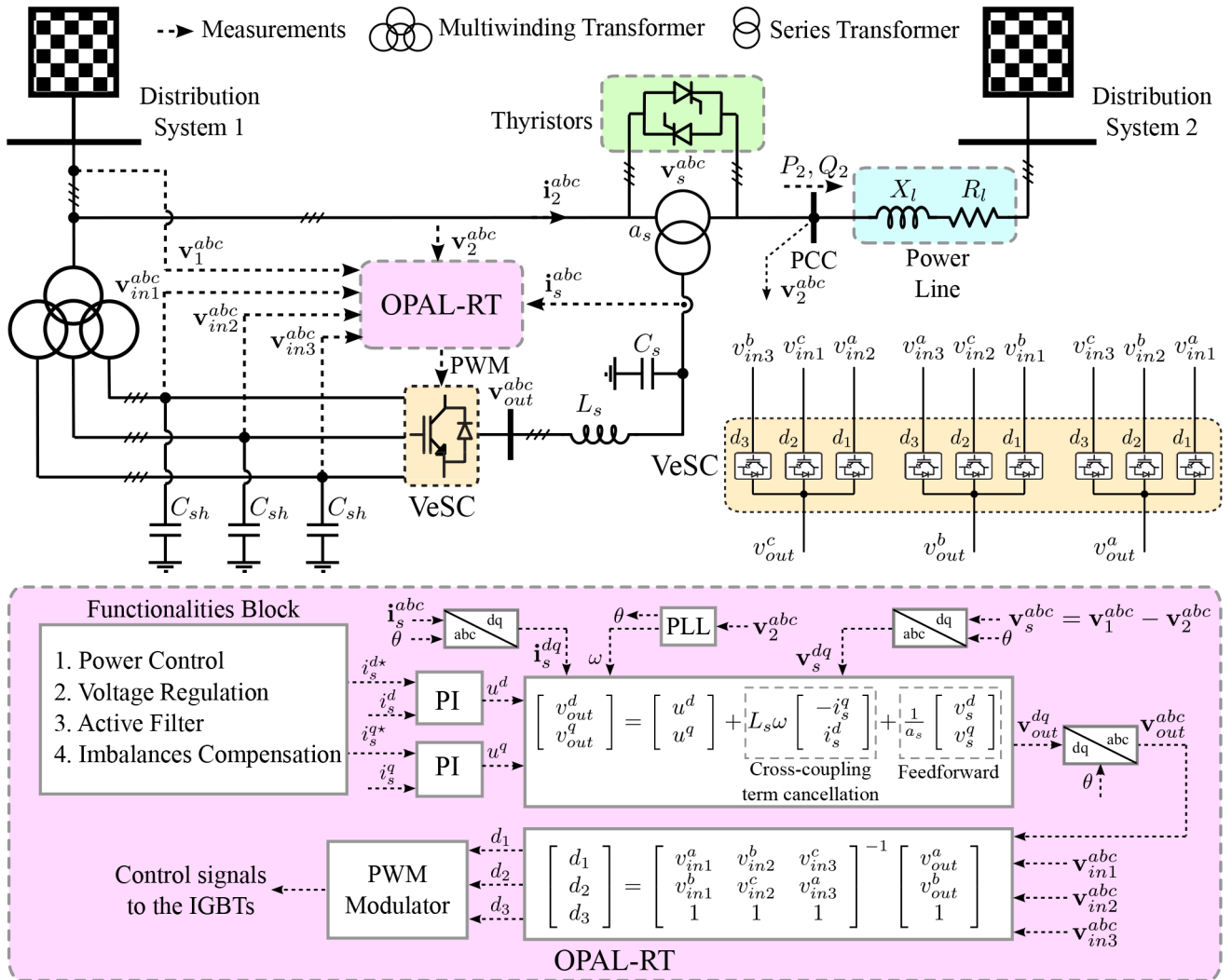
Fig. 1 *Top: Single-phase circuit schematic of the ac-link ShSPFC based on the experimental prototype. Bottom: Feedback linearisation control strategy implemented in a real-time platform OPAL-RT*

control is essential for any higher control level devoted to providing advanced functionalities such as power flow control, voltage regulation or harmonic and imbalance compensation. As depicted in Fig. 1, these functionalities block will provide the current references $i_s^{d\star}$ and $i_s^{q\star}$ to the closed-loop current controller addressed in this paper. The reference current computation by the functionalities block is not within the scope of this paper and will be investigated in future studies.

The remaining of the paper is organised as follows. Section 2 presents the ac-link ShSPFC experimental prototype assembled in the laboratory to validate the current control loop. Section 3 depicts and discusses the performance of the controller via experimental results for the steady-state and transient regime. Finally, the conclusions of Section 4 close the paper.

2 Ac-link ShSPFC experimental prototype

This section describes the experimental prototype of the ac-link ShSFC used to validate the feedback linearisation control strategy. The experimental setup assembled in the laboratory is depicted in Fig. 2, which follows the single-phase circuit schematic shown on the top of Fig. 1. The relevant parameters of the system are collected in Table 1. Basically, this setup consists of one VeSC connecting two points of the laboratory low voltage network through a series transformer and an impedance, R_l and X_l, which emulates a power line. The VeSC input is connected to a multi-winding transformer consisting of a primary winding and three secondary windings all connected in star. Additionally, ac capacitors are added to the VeSC input, C_{sh}, and an LC filter, L_s and C_s, connected to the output in order to improve the power

quality of the voltage and current generated by the converter. Connecting a series transformer requires additional security protections. In the event that the secondary of this transformer remains open, an overvoltage may occur damaging the series transformer and the VeSC. To avoid this problem, a group of thyristors are connected in parallel with the series transformer. These are responsible for short-circuiting the secondary side of the series transformer when the VeSC is not working or in the event of a fault in the system.

Voltages, $[v_1^{abc}, v_2^{abc}, v_{in1}^{abc}, v_{in2}^{abc}, v_{in3}^{abc}]$, and currents, i_s^{abc}, are measured using voltage transducers LV-25P and current transducers HAS 50-S, respectively. These measurements are centralised in an interface board, guaranteeing adequate isolation and shielding, which is connected to the analogue inputs of a real-time controller developed by OPAL-RT Technologies. Note that v_s^{abc} is computed from v_1^{abc} and v_2^{abc} as depicted in Fig. 1 to reduce the number of transducers in the prototype. The control strategy depicted on the block diagram at the bottom of Fig. 1 is executed every 50 µs to compute a set of duty ratios d_{123}. These output magnitudes are transformed into switching signals after applying a PWM technique described in [8]. These output switching signals are directly connected to the VeSC IGBT drivers using the high-frequency optical digital outputs available in the OPAL-RT platform.

3 Ac-link ShSPFC experimental results

The performance of the controller is evaluated on the experimental prototype in steady and transient states. In addition, a comparison
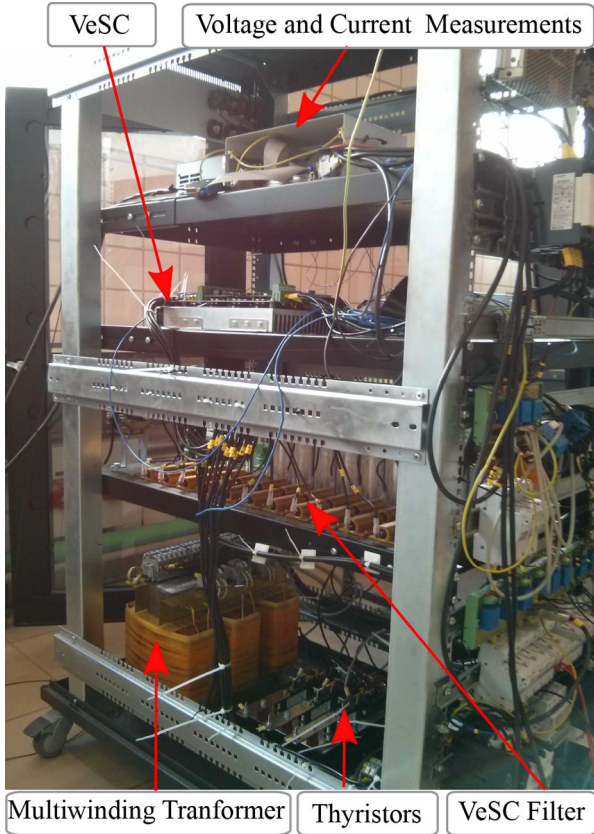
Fig. 2 *Photo of the laboratory experimental test bench*

Table 1 Parameter of the experimental ac-link ShSPFC

ac-link ShSPFC parameter	Actual value
low voltage laboratory network	400 V
rated power of systems 1 and 2	20 kVA
multi-winding transformer	Yy0y0y0
multi-winding transformer rated voltages	400/170/170/170 V
multi-winding transformer rated power	15.5/4.5/4.5/4.5 kVA
series transformer connection group	Y/open winding
series transformer rated voltages	100/50 V
series transformer rated power	4.5/1.5/1.5/1.5 kVA
VeSC rated current/voltage	30 A/100 V
VeSC switching frequency	5 kHz
input capacitance filter C_{sh}	30 µF
output filter L_s/C_s	1.1 mH/10 µF
line R_l/X_l	0.086 Ω/0.125 Ω

is made between simulation and experimental results in a steady state.

3.1 Steady-state performance

The steady-state performance is evaluated using the following current references: $i_s^{d\star} = 7\,\text{A}$ and $i_s^{q\star} = -7\,\text{A}$. These setpoints have been selected because they correspond to a half of the ac-link ShSPFC rated power, being acceptable values to study the harmonic content of the currents. The currents in the *abc* coordinates are illustrated in Fig. 3, where the top and bottom plots present simulated and experimental waveforms, respectively. Note that the peak value of the currents must be equal to $\sqrt{i_s^{d^2} + i_s^{q^2}}$ which is $\sqrt{98}$ according to the references. This is in consonance with the simulation and experimental results depicted in Fig. 3. In addition, it is also important to highlight that the simulation and experimental currents are practically in phase considering the same voltage reference. The only main difference between these results is that the experimental currents are distorted due to the voltage
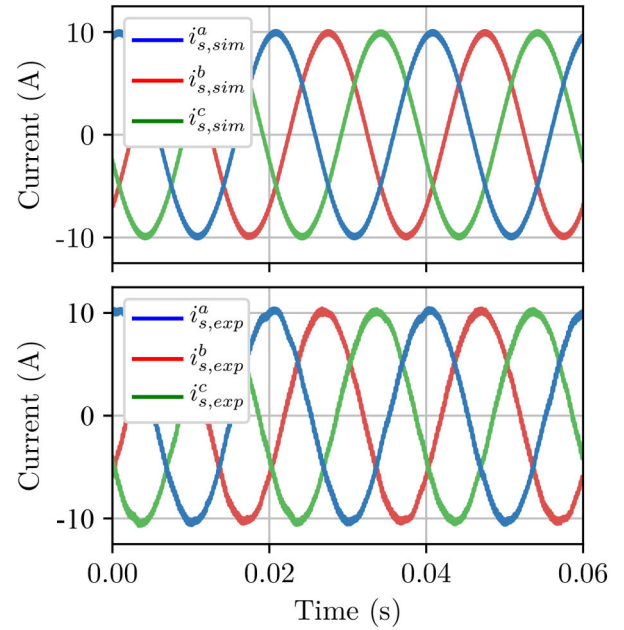

Fig. 3 *Steady-state currents i_s^{abc}. Top: Simulated waveforms. Bottom: Experimental waveforms*
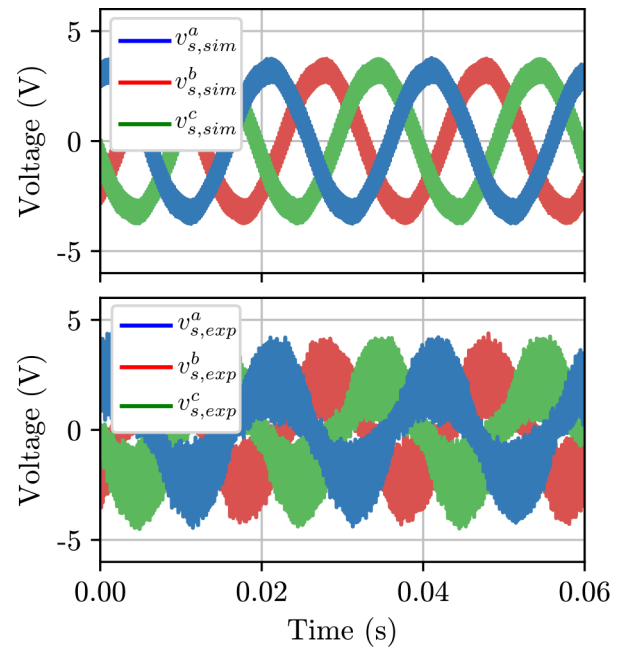

Fig. 4 *Steady-state voltages v_s^{abc}. Top: Simulated waveforms. Bottom: Experimental waveforms*

harmonic distortion of the laboratory network. However, the total harmonic distortion of the current remains below 2.9%, which can be considered as usual in this kind of power electronic applications.

The series voltages injected by the VeSC ShSPFC to achieve the reference currents are shown in Fig. 4. Again, there is a good matching between the simulated and experimental results in the peak and phase values of these magnitudes. However, it can be noticed a higher frequency harmonic content in the voltages generated by the experimental results due to the non-ideal switching of the actual prototype IGBTs.

Finally, the duty ratios computed by the current control loop are shown in Fig. 5 is possible to notice the similarity between simulation and experimental results. The difference between them is the oscillation that appears in the experimental duty ratios due to the harmonic content of the input voltages $[v_{in1}^{abc}, v_{in2}^{abc}, v_{in3}^{abc}]$, which are proportional to the laboratory network voltage.
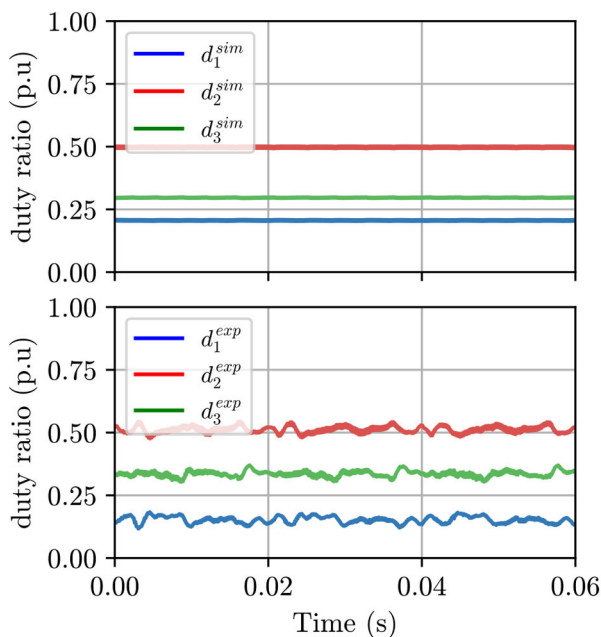
Fig. 5 *Steady-state duty ratios* $[d_1, d_2, d_3]$. *Top: Simulated waveforms. Bottom: Experimental waveforms*

3.2 Transient-state performance

This subsection presents the transient response of the feedback linearisation controller for a step change on the reference current. Initially, the reference currents $i_s^{d\star}$ and $i_s^{q\star}$ are set to zero and after that $i_s^{d\star}$ is changed to 5 A.

The top plot of Fig. 6 shows the reference and measured currents, $i_s^{dq\star}$ and i_s^{dq}, respectively, injected by the VeSC. As expected, a first-order dynamic response and good tracking of i_s^d occurs according to the designed control strategy. In addition, the system presents a high degree of decoupling since i_s^q is hardly disturbed when the reference current $i_s^{d\star}$ changes.

Finally, the evolution of i_s^{abc} and v_s^{abc} is also shown in Fig. 6. Note that the currents are null initially according to the established reference. After the reference change, the currents evolve exponentially until reaching a steady state with a peak value of 5 A. In the same way, the voltage v_s^{abc} injected by the series transformer evolves with a first-order dynamics.

4 Conclusion

Experimental validation of a current control loop using feedback linearisation for an ac-link ShSPFC has been presented in this paper. The objective is to control the currents i_s^d and i_s^q transferred between two interconnected systems linked by this device. The validation of this control loop is key to assure new functionalities provided by additional high-level control algorithms such as regulation of active and reactive power flows between both systems, PCC voltage support and imbalanced and harmonic mitigation.

The experimental results allow us to validate the control algorithm due to the excellent matching with the simulations in terms of currents, series voltages and duty ratios. These good results have been obtained both in steady-state and transient conditions where a controlled first-order dynamic with uncoupling of the *dq* components has been achieved.

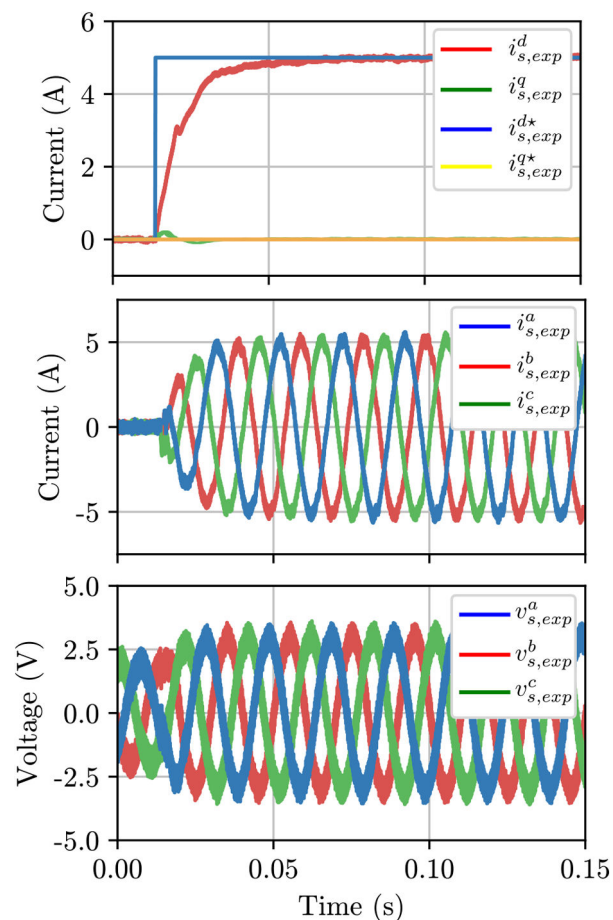## 5 Acknowledgment

Fig. 6 *Top: Transient-state currents* $i_s^{dq\star}$ *and* i_s^{dq}. *Middle: Transient-state current* i_s^{abc}. *Bottom: Transient-state voltage* v_s^{abc}

6 References

[1] Chakraborty, C., Iu, H.H.C., Lu, D.D.C.: 'Power converters, control, and energy management for distributed generation', *IEEE Trans. Ind. Electron.*, 2015, **62**, (7), pp. 4466–4470

[2] Johal, H., Divan, D.: 'Design considerations for series-connected distributed FACTS converters', *IEEE Trans. Ind. Electron.*, 2007, **43**, (6), pp. 1609–1618

[3] Maza-Ortega, J.M., Gómez-Expósito, A., Barragán-Villarejo, M., *et al.*: 'Voltage source converter-based topologies to further integrate renewable energy sources in distribution systems', *IET Renew. Power Gener.*, 2012, **6**, (6), pp. 435–445

[4] Tang, C., Chen, Y., Chen, Y., *et al.*: 'Dc-link voltage control strategy for three-phase back-to-back active power conditioners', *IEEE Trans. Ind. Electron.*, 2015, **62**, (10), pp. 6306–6316

[5] Lozano-García, J.M., Ramirez, J.M.: 'Voltage compensator based on a direct matrix converter without energy storage', *IET Power Electron.*, 2015, **8**, (3), pp. 321–332

[6] Kewat, S., Singh, B.: 'Modified amplitude adaptive control algorithm for power quality improvement in multiple distributed generation system', *IET Power Electron.*, 2019, **12**, (9), pp. 2321–2329

[7] Mancilla-David, F., Battacharya, S., Venkataramanan, G.: 'A comparative evaluation of series power-flow controllers using dc- and ac-link converters', *IEEE Trans. Power Deliv.*, 2008, **23**, (2), pp. 985–996

[8] Barragán-Villarejo, M., Venkataramanan, G., Mancilla-David, F., *et al.*: 'Dynamic modelling and control of a shunt-series power flow controller based on AC-link', *IET Gener. Transm. Distrib.*, 2012, **6**, (8), pp. 792–802

[9] Barragán-Villarejo, F., Marano-Marcolini, A., Maza-Ortega, J.M., *et al.*: 'Steady-state model for the three-leg shunt-series ac-link power flow controller', *IET Gener. Transm. Distrib.*, 2015, **9**, (16), pp. 2534–2543

[10] Ajami, A., Mohajel Kazemi, F.: 'Power flow controlling using SSSC based on matrix converter via SA-PSO algorithm', *Turkish J. Electr. Eng. Comput. Sci.*, 2016, **24**, (3), pp. 1461–1473

[11] Yazdani, A., Iravani, R.: '*Voltage-sourced converters in power systems*' (Wiley, USA, 2010)

[12] Garcia-Vite, P.M., Mancilla-David, F., Ramirez, J.M.: 'Per-sequence vector-switching matrix converter modules for voltage regulation', *IEEE Trans. Ind. Electron.*, 2013, **60**, (12), pp. 5411–5421